The Science of Nature (2018) 105:28
https://doi.org/10.1007/s00114-018-1548-y

ORIGINAL PAPER

Phylogenetic and functional implications of the ear region anatomy of *Glossotherium robustum* (Xenarthra, Mylodontidae) from the Late Pleistocene of Argentina

Alberto Boscaini[1] · Dawid A. Iurino[2,3] · Guillaume Billet[4] · Lionel Hautier[5] · Raffaele Sardella[2,3] · German Tirao[6] · Timothy J. Gaudin[7] · François Pujos[1]

Received: 28 November 2017 / Revised: 21 February 2018 / Accepted: 23 February 2018

Abstract

Several detailed studies of the external morphology of the ear region in extinct sloths have been published in the past few decades, and this anatomical region has proved extremely helpful in elucidating the phylogenetic relationships among the members of this mammalian clade. Few studies of the inner ear anatomy in these peculiar animals were conducted historically, but these are increasing in number in recent years, in both the extinct and extant representatives, due to wider access to CT-scanning facilities, which allow non-destructive access to internal morphologies. In the present study, we analyze the extinct ground sloth *Glossotherium robustum* and provide a description of the external features of the ear region and the endocranial side of the petrosal bone, coupled with the first data on the anatomy of the bony labyrinth. Some features observable in the ear region of *G. robustum* (e.g., the shape and size of the entotympanic bone and the morphology of the posteromedial surface of the petrosal) are highly variable, both intraspecifically and intraindividually. The form of the bony labyrinth of *G. robustum* is also described, providing the first data from this anatomical region for the family Mylodontidae. The anatomy of the bony labyrinth of the genus *Glossotherium* is here compared at the level of the superorder Xenarthra, including all available extant and extinct representatives, using geometric morphometric methods. In light of the new data, we discuss the evolution of inner ear anatomy in the xenarthran clade, and most particularly in sloths, considering the influence of phylogeny, allometry, and physiology on the shape of this highly informative region of the skull. These analyses show that the inner ear of *Glossotherium* more closely resembles that of the extant anteaters, and to a lesser extent those of the giant ground sloth *Megatherium* and euphractine armadillos, than those of the extant sloths *Bradypus* and *Choloepus*, further demonstrating the striking morphological convergence between the two extant sloth genera.

Keywords *Glossotherium* · Ground sloth · Ear region · Bony labyrinth · Phylogeny · Function

Communicated by: Sven Thatje

Electronic supplementary material The online version of this article (https://doi.org/10.1007/s00114-018-1548-y) contains supplementary material, which is available to authorized users.

✉ Alberto Boscaini
aboscaini@mendoza–conicet.gob.ar

[1] Instituto Argentino de Nivología, Glaciología y Ciencias Ambientales (IANIGLA), CCT-CONICET-Mendoza, Avda. Ruiz Leal s/n, Parque Gral. San Martín, 5500 Mendoza, Argentina

[2] Dipartimento di Scienze della Terra, Sapienza Università di Roma, Piazzale A. Moro 5, 00185 Rome, Italy

[3] PaleoFactory, Sapienza Università di Roma, Piazzale A. Moro 5, 00185 Rome, Italy

[4] Centre de Recherche sur la Paléobiodiversité et les Paléoenvironnements (CR2P), UMR CNRS 7207, MNHN, Sorbonne Universités, CP 38, Muséum national d'Histoire naturelle, 8 rue Buffon, 75005 Paris, France

[5] Institut des Sciences de l'Evolution, CNRS, IRD, EPHE, Université de Montpellier, F-34095 Montpellier, France

[6] IFEG (CONICET), Facultad de Matemática, Astronomía y Física, Universidad Nacional de Córdoba, Haya de la Torre y Medina Allende, X5000HUA Córdoba, Argentina

[7] Department of Biology, Geology, and Environmental Science, University of Tennessee at Chattanooga, 615 McCallie Ave, Chattanooga, TN 37403-2598, USA

Published online: 27 March 2018

Abbreviations

FMNH	Field Museum of Natural History (Chicago, USA)
FUESMEN	Fundación Escuela de Medicina Nuclear (Mendoza, Argentina)
MACN Pv	Colección de Paleontología de Vertebrados, Museo Argentino de Ciencias Naturales "Bernardino Rivadavia" (Buenos Aires, Argentina)
MLP	División Paleontología de Vertebrados, Museo de La Plata (La Plata, Argentina)
ROM	Royal Ontario Museum (Toronto, Canada)

Introduction

The clade Folivora (= Tardigrada = Phyllophaga; Delsuc et al. 2001; Fariña and Vizcaíno 2003) comprises all the extant and extinct sloths, and is represented in the fossil record of the Americas by hundreds of species (Mones 1986; McKenna and Bell 1997), in contrast with the reduced diversity of their extant relatives, which encompasses only six species. According to Gaudin and Croft (2015) the first sloth remains date back to the late Eocene. Over their long history, extinct sloths have occupied a great number of ecological niches, as demonstrated by their marked variability in locomotory modes (with facultative bipeds, obligate quadrupeds, arboreal and semiarboreal taxa, and even some swimming taxa; Pujos et al. 2012; Toledo 2016) and in dietary habits (with browsers, grazers, and mixed feeders; Bargo et al. 2006; Bargo and Vizcaíno 2008; Pujos et al. 2012). The family Mylodontidae, which includes the species considered in this study, *Glossotherium robustum* (Owen, 1842), is one of the first two families of sloths (with Megalonychidae) to appear during the late Oligocene (Pujos and De Iuliis 2007). Mylodontids included a large number of mainly quadrupedal and grazing/browsing genera that persisted until the late Pleistocene/earliest Holocene periods (Pujos et al. 2012, 2017; Gaudin and Croft 2015; Slater et al. 2016).

By contrast, extant sloths are represented by only two genera: *Bradypus* Linnaeus, 1758 and *Choloepus* Illiger, 1811, and are almost exclusively arboreal and folivorous animals (Pujos et al. 2012). Their peculiar upside-down posture and suspensory behavior were independently acquired in both lineages, and considered one of the most striking examples of convergence among mammals (Gaudin 1995, 2004; Nyakatura 2012; Pujos et al. 2012, 2017). Even if the exact phylogenetic position of the extant sloths is still highly debated, the diphyly of the two genera is confirmed by several phylogenetic analyses, based on both morphological and molecular evidence (Gaudin 1995, 2004; Greenwood et al. 2001; Clack et al. 2012; Slater et al. 2016).

From a morphological point of view, the external ear region of extinct sloths has proved to be an important source of information, providing diagnostic features which have been useful in clarifying phylogenetic relationships (e.g., Patterson et al. 1992; Gaudin 1995, 2004). Indeed, De Iuliis (2017) has recently drawn attention to both the importance of the ear region in this regard and the need for increased rigor in treating this region in descriptions of new xenarthran taxa. Detailed anatomical descriptions of this skull region date back to the first description of fossils sloths in the nineteenth century (e.g., Owen 1842), but have become more prevalent during the last few decades (e.g., Patterson et al. 1992; Gaudin 1995, 2011; De Iuliis et al. 2011; Gaudin et al. 2015).

Previous studies of the ear region in *Glossotherium robustum*, however, are either outdated or incomplete. The early descriptions by Owen (1842), van der Klaauw (1931) and Guth (1961) were pioneering works in their time, but suffered from erroneous taxonomic attribution (for a summary of the chaotic taxonomic history of the genus *Glossotherium*, see Esteban 1996; Fernicola et al. 2009; McAfee 2009; De Iuliis et al. 2017), as well as old terminology and a lack of detail. More recently, Patterson et al. (1992) provided descriptions of the ear region in a wide variety of extinct and extant sloths, but only marginally considered the genus *Glossotherium*, whose description was coupled to that of the North American genus *Paramylodon*. Moreover, Patterson et al. (1992) and Gaudin (1995, 2004) based their observations of *Glossotherium* on a single skull housed in the Field Museum of Natural History of Chicago (FMNH 14204) from the Tarija Valley of Bolivia, assigned by some authors to *Glossotherium tarijensis* Ameghino 1902 (see Pitana et al. 2013 and Pujos et al. 2017). Given that the validity of the latter species has never been properly established, we provide a detailed description of the ear region in some undoubted *G. robustum* specimens from Argentina, which should help to clarify the alpha taxonomy of the genus. In fact, a detailed revision of the genus *Glossotherium*, together with an independent codification of its species, is currently underway. Given the great importance of characters from the ear region in past phylogenetic analyses of sloths (e.g., Gaudin 1995, 2004), understanding the morphology and the intraspecific variation of ear region features of *G. robustum* is fundamental in order to reconstruct the phylogenetic relationships at the species level.

Besides phylogeny, the external anatomy of the ear region has also been useful in revealing some aspects of the palaeobiology of Pleistocene ground sloths, such as their hearing capabilities. For example, based on the area of the ectotympanic and the form of the middle ear ossicles, Blanco and Rinderknecht (2008, 2012) suggested that giant mylodontid sloths such as *Glossotherium* and *Lestodon* were particularly sensitive to low-frequency sounds.

Studies on the inner ear of extinct xenarthrans are limited, but important advances have been made in the last few years. The only bony labyrinth of an extinct sloth described to date is

that of *Megatherium,* which shows a peculiar morphology, very different from those of extant sloths and more similar to that of the extant armadillos and anteaters (Billet et al. 2013). Billet et al. (2015a), in an extended database, studied the effect of allometry and the phylogenetic information contained in the morphology of the xenarthran inner ear (mostly extant taxa), using morphometric analyses based on 3D landmarks data. Finally, Coutier et al. (2017) analyzed and discussed a possible relationship between the orientation of the lateral semicircular canal and the usual position of the head in their sample of xenarthrans, which included two extinct sloths (*Megatherium* and *Pelecyodon*).

In fact, the morphology of this particular anatomical region is strongly influenced by both phylogeny and function (Ekdale 2013, 2016). The cochlea is strictly related to the sense of hearing, whereas the vestibule and the semicircular canals are associated with the sense of balance and equilibrium (Ekdale 2016). In recent years, several aspects of the shape, size, and orientation of the bony labyrinth in mammals have been linked to physiological features. For instance, the size of the semicircular canals correlates with body mass and agility categories (Spoor et al. 2007; Silcox et al. 2009). In addition, the angles among the semicircular canals has been associated with vestibular sensitivity (Malinzak et al. 2012; Berlin et al. 2013), and the shape of the cochlea with the lower frequency hearing limits (Manoussaki et al. 2008).

These analyses have also been tentatively applied to extinct animals, with the aim to infer functional aspects from inner ear morphology (e.g., Orliac et al. 2012; Macrini et al. 2013; Ekdale and Racicot 2015). However, these methodologies have also been criticized by several authors, who found the proposed methods partly unreliable or difficult to replicate (e.g., David et al. 2010, 2016; Billet et al. 2013; Danilo et al. 2015; Orliac and O'Leary 2016; Perier et al. 2016; Ruf et al. 2016).

The aims of the present work are to provide a detailed description of the basicranial region of *G. robustum*, coupled with the first digital reconstructions of a mylodontid petrosal and bony labyrinth. The shape of the bony labyrinth of *G. robustum* is here compared with the available xenarthran dataset, in order to discuss phylogenetic and allometric aspects of this peculiar anatomical region in sloths, and is complemented by a brief discussion of its possible functional attributes.

Materials and methods

Specimens studied and data processing

The description of external ear region anatomy is based on two specimens of *Glossotherium robustum*: MACN Pv 13553 (Supplementary Information S1) and MLP 3–136 (Supplementary Information S2). The first specimen is an undescribed neurocranium found in 1933 in the vicinity of Tandil (Buenos Aires Province, Argentina). The second is a complete skull, originally described and figured by Lydekker (1894) [p.78–80, plates XLVIII-XLIX(2)-LII(1)].

For logistical reasons, only the neurocranium of MACN Pv 13553 was transported to the city of Mendoza, where it was scanned using the General Electric Lightspeed CT scanner in the FUESMEN Institute. The scanning resulted in 839 slices with a thickness of 0.62 mm. The image segmentation process was performed using OsiriX v.5.6 and Materialise Mimics v.17 software. Both the left and right bony labyrinths were digitally reconstructed, both of them being slightly damaged at the level of the lateral semicircular canal. However, the trajectory of the latter canal was still strongly marked on the petrosal and a reliable reconstruction was obtained. The description and comparison is based on the right labyrinth, but, given the similarity between the two sides, is valid for both. Linear and angular measurements of the bony labyrinths were taken using the 3D measurement tools of Mimics v.17 and AVIZO (Supplementary Information S3).

Morphometric comparisons of the bony labyrinth

The 3D reconstruction of the bony labyrinth of *G. robustum* MACN Pv 13553 was compared to the database of Billet et al. (2015a), composed of 40 adult xenarthran specimens, and representing 13 extant genera (including living sloths, armadillos and anteaters) and the extinct ground sloth *Megatherium*. Following Billet et al. (2015a), 80 semilandmarks were digitized on the bony labyrinth of *G. robustum* with the interactive software ISE-MeshTools (Lebrun 2014). The semilandmarks were equally distributed on the three semicircular canals and the cochlea, and the digitization was conducted using the same operator as in Billet et al. (2015a) (G.B.) in order to minimize interobserver errors. Analysis and visualization of shape variation patterns were conducted using the interactive software package MORPHOTOOLS (Specht 2007; Specht et al. 2007; Lebrun 2008; Lebrun et al. 2010).

The principal component analyses (PCA) were conducted alternatively with and without correction of the shape data for allometry, using either body mass values or centroid size of the inner ears as estimators of size. The estimated body mass for *G. robustum* (1216 kg) was taken from Fariña et al. (1998), the same source used by Billet et al. (2013, 2015a) for the body mass estimation of *Megatherium*. Both the estimators, body mass and centroid size of the inner ear, were also used as external variables so as to obtain the respective allometric shape vectors (ASV). An allometric shape vector represents a direction in shape space, which characterizes the main transformations related to size changes. A partial least squares (PLS) analysis was also performed using the landmark configurations of the semicircular canals and the cochlea as distinct blocks, in order to assess the morphological features that

covary between them (for more detailed information on the applied methods, see Billet et al. 2015a).

Functional aspects/attributes of the bony labyrinth

In an attempt to explain the peculiar morphology of the bony labyrinth in *G. robustum* that emerged from the morphometric geometric analyses (see "Results"), we tried to replicate studies that have been proposed in recent years, relating the shape of labyrinthine features to functional aspects (e.g., Spoor et al. 2007; Manoussaki et al. 2008; Silcox et al. 2009; Malinzak et al. 2012; Berlin et al. 2013). However, in doing so, we took into account the criticisms that other authors have offered on the accuracy and reliability of these methods (e.g., David et al. 2010, 2016; Malinzak et al. 2012; Billet et al. 2013; Danilo et al. 2015; Orliac and O'Leary 2016; Perier et al. 2016; Ruf et al. 2016). For example, the a priori agility categories established by Spoor et al. (2007) correspond to subjective impressions according to Malinzak et al. (2012), whereas Billet et al. (2013) and Ruf et al. (2016) demonstrated the difficulty of using the equations of Silcox et al. (2009) for extremely large and small-sized taxa. For this reason, we plotted the semicircular canal ratio (SCR) value over the body mass estimation of the *G. robustum* specimen MACN Pv 13553, in order to visualize it in the mammalian graphs published by Spoor et al. (2007: Fig. 1b), but opted not to use the predictive agility equations of Silcox et al. (2009).

The studies of Malinzak et al. (2012) and Berlin et al. (2013) related the average deviation from orthogonality of the ipsilateral semicircular canals with the pattern of locomotor head movements and the average sensitivity of the semicircular canals. Both studies, however, fail to consider intraspecific variation and have quite low regression correlation coefficients (Ruf et al. 2016). The deviation from orthogonality of the ipsilateral semicircular canals in *Glossotherium* (90_{var} sensu Berlin et al. 2013) is nevertheless calculated here, but is discussed in the context of Ruf et al.'s (2016) critiques.

In both marine and terrestrial mammals, the radii ratio of the cochlea (calculated as the ratio between the radius of the basal turn and the radius of the apical turn of the cochlea) is linearly correlated with the lower limit of low-frequency hearing abilities (Manoussaki et al. 2008). Following the procedure of Manoussaki et al. (2008), we calculated the radii of curvature for the basal and apical cochlear turns. Their ratio was used in the equation:

$$f = 1.507\ exp\ [0.578\ (p-1)]$$

where f = low-frequency hearing limit and p = radii ratio = R_{base}/R_{apex}, in order to predict the low-frequency hearing limit for *G. robustum*. This approach was criticized by Danilo et al. (2015), Ekdale and Racicot (2015), and Orliac and O'Leary (2016), who experienced problems in repeating the protocol.

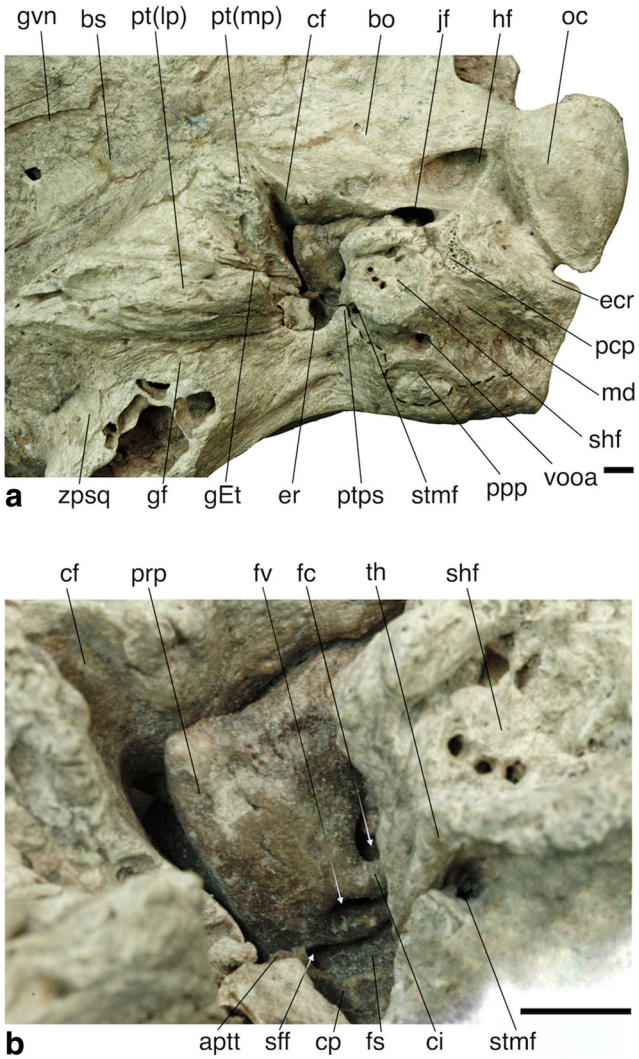

Fig. 1 External ear region (**a**) and detail of the petrosal region (**b**) of *Glossotherium robustum* (MACN Pv 13553) in ventrolateral view (anterior towards the left). Abbreviations: aptt, anteroventral process of the tegmen tympani; bo, basioccipital; bs, basisphenoid; cf, carotid foramen; ci, crista interfenestralis; cp, crista parotica; ecr, exoccipital crest; er, epitympanic recess; fc, fenestra cochleae (= fenestra rotunda); fs, facial sulcus; fv, fenestra vestibuli (= fenestra ovalis); gEt, groove for the Eustachian tube; gf, glenoid fossa; gvn, groove for the vidian nerve; hf, hypoglossal foramen; jf, jugular foramen; md, mastoid depression; oc, occipital condyle; pcp, paracondylar process of exoccipital (= paraoccipital process of Patterson et al. 1992); ppp, paraoccipital process of petrosal (= mastoid process of squamosal of Patterson et al. 1992); prp, promontorium of petrosal; pt(lp), pterygoid (lateral portion); pt(mp), pterygoid (medial portion); ptps, posttympanic process of squamosal; sff, secondary facial foramen; shf, stylohyal fossa; stmf, stylomastoid foramen; th, tympanohyal; vooa, ventral opening for the occipital artery (= mastoid foramen of Patterson et al. 1992); zpsq, zygomatic process of squamosal. Scale bars equal 1 cm

We observed the same difficulties and, therefore, provide a range of values (minimum and maximum) obtained independently by two of us (A.B. and D.A.I). The results have been coupled with observations of cochlear morphological features that have been previously linked with hearing abilities in mammals (for a summary see Ekdale 2016).

Results

Systematic paleontology

Superorder XENARTHRA Cope, 1889
Order PILOSA Flower, 1883
Suborder FOLIVORA Delsuc et al., 2001
Family MYLODONTIDAE Gill, 1872
Subfamily MYLODONTINAE Gill, 1872
Genus *Glossotherium* Owen, 1840
Glossotherium robustum (Owen, 1842)

Referred material MACN Pv 13553, neurocranium (Fig. 1; Supplementary Information S1); MLP 3–136, cranium and mandible with complete dentition (Fig. 2; Supplementary Information S2).

Stratigraphic and geographic occurrence MACN Pv 13553, Upper Pampean Formation (Late Pleistocene), Tandil, Buenos Aires province, Argentina; MLP 3–136, Pampean Formation (Pleistocene), Buenos Aires province, Argentina.

Description of the ear region

MACN Pv 13553 comprises the posterior portion of a *Glossotherium robustum* skull (Supplementary Information S1). The anterior part of the skull and the skull roof are lacking, exposing the air spaces that form the sinuses surrounding the braincase dorsally and anteriorly. The zygomatic processes of the squamosals are also broken at their bases. In contrast, the ventral and occipital portions of the skull are well preserved, and it is possible to observe the majority of the anatomical features of the ear region (Fig. 1). The ecto- and entotympanic bones are missing, exposing the middle ear cavity and much of the ventral part of the petrosal (Fig. 1). However, both the ecto- and entotympanic bones are well preserved in MLP 3–136 (Fig. 2), and their description is consequently based on this specimen.

Ectotympanic Only the left ectotympanic of MLP 3–136 is preserved (Fig. 2). In lateral view, it appears thickened transversely and elongated dorsoventrally, the latter a typical xenarthran condition (Fig. 2) (Patterson et al. 1989; Patterson et al. 1992; Gaudin 1995, 2011). This bone has a smooth external surface, a common mylodontid feature according to Gaudin (1995: char. 1). In lateral view, the incisura tympanica is interposed between the dorsal ends of the bowed anterior and posterior crura (Fig. 2b). The former is connected anteriorly to the lateral portion of the pterygoid and dorsally to the squamosal, whereas the latter is dorsally sutured to the superficies meatus/post-tympanic process of the squamosal. Among the mylodontids, the tympanic-pterygoid contact is considered an autopomorphic trait in the genus *Glossotherium* (Gaudin 1995: char. 10). In ventral view (Fig. 2a), the ectotympanic is anteromedially oriented and is shorter anteroposteriorly than the entotympanic. In this specimen, the ectotympanic does not show any contact with the entotympanic, a condition also present in *Paramylodon* and *Lestodon,* whereas a weak anterior connection is observed in other genera of the family Mylodontidae (Gaudin 1995: char 12).

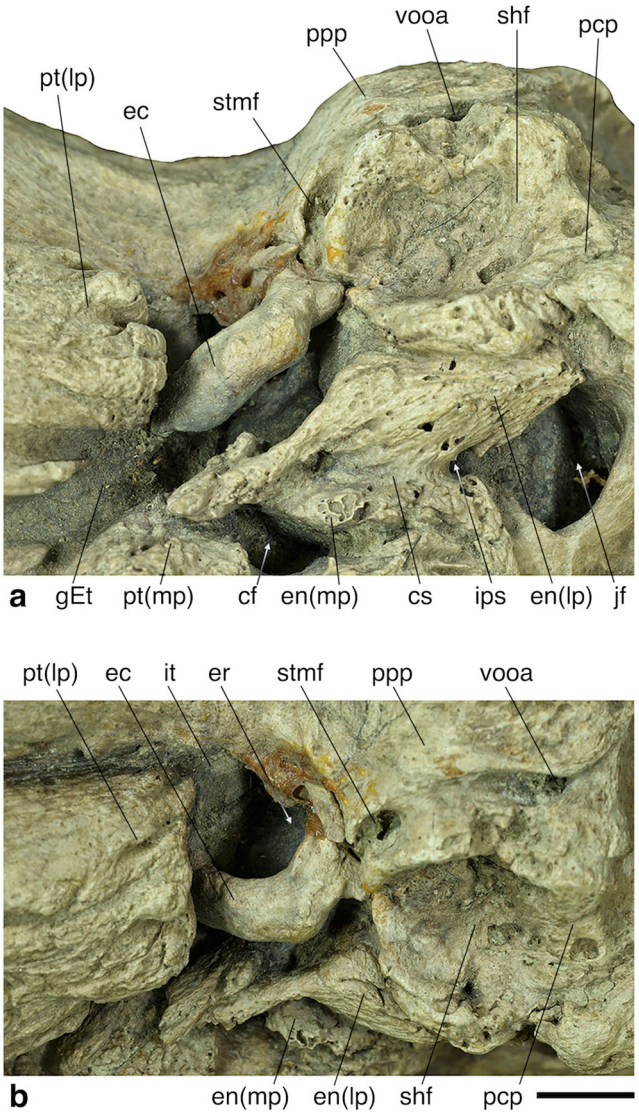

Fig. 2 External ear region in *Glossotherium robustum* (MLP 3–136) in ventral (**a**) and ventrolateral (**b**) views (anterior towards the left). Abbreviations: cf, carotid foramen; cs, carotid sulcus; ec, ectotympanic; en(lp), entotympanic (lateral plate); en(mp), entotympanic (medial plate); er, epitympanic recess; gEt, groove for the Eustachian tube; ips, inferior petrosal sinus; it, incisura tympanica; jf, jugular foramen; pcp, paracondylar process of exoccipital (= paraoccipital process of Patterson et al. 1992); ppp, paraoccipital process of petrosal (= mastoid process of squamosal of Patterson et al. 1992); pt(lp), pterygoid (lateral portion); pt(mp), pterygoid (medial portion); shf, stylohyal fossa; stmf, stylomastoid foramen; vooa, ventral opening for the occipital artery (= mastoid foramen of Patterson et al. 1992). Scale bar equals 1 cm

Entotympanic Both entotympanic bones are present in MLP 3–136. The entotympanic is a blocky structure, more massive

posteriorly than anteriorly, narrowing rostrally, and directed medially and ventrally. It is divided into medial and lateral plates. The latter is in turn separated into anterior and posterior parts by a broad "v-shaped" notch in its ventral edge (Fig. 2b). The carotid sulcus divides the medial and the lateral entotympanic plates. The sulcus itself is pierced by two foramina. The anterior one probably transmitted a branch of the internal carotid artery supplying the entotympanic and tympanic cavity, whereas the posterior one housed the inferior petrosal sinus (Fig. 2). In *Mylodon*, the roof of the carotid sulcus is also pierced by two foramina. Both lead to the tympanic cavity (Patterson et al. 1992), making the homology of the more posterior foramen in *Mylodon* with the inferior petrosal sinus foramen in MLP 3–136 doubtful. However, the anterior foramen seems to be homologous in the two genera, because they both lead to the tympanic cavity and probably transmitted a branch of the internal carotid artery.

The entotympanic contributes to the roof and the lateral and medial walls of the carotid sulcus (Fig. 2a). This sulcus opens ventrally, without any floor formed by the entotympanic, reflecting the absence of a carotid canal (sensu Gaudin 2011). The medial plate of the entotympanic is shorter than the lateral plate, as described also for *G. tropicorum* by De Iuliis et al. (2017), and is fused medially and posteriorly with the basioccipital, as in *Mylodon* (Patterson et al. 1992). The medial plate lies in a parasagittal plane and is quite uniform in transverse width, without the posterior enlargement described in *Mylodon* (Patterson et al. 1992). Its anterior margin contributes to the posterior margin of the carotid foramen. The remainder of the carotid foramen is formed laterally by the lateral plate of the entotympanic, anteriorly by the medial portion of the pterygoid and medially by the anterior edge of the basisphenoid/basioccipital tuber (Fig. 2a).

The extended anteroventral process of the lateral plate of the entotympanic is not common in mylodontid sloths (Gaudin 1995: char 21), but in MLP 3–136 it is present, and more medially directed than in *Mylodon* (Patterson et al. 1992). Its anterior margin contacts the medial portion of the pterygoid, and is fused dorsally to the ventral part of the promontorium, building a lateral wall involved in the formation of the tympanic cavity wall (Fig. 2b). The posterior part of the lateral plate of the entotympanic is triangular in shape, broad transversely, with an anteroposteriorly directed ventral enlargement. It is in contact posteriorly with the paracondylar process of the exoccipital, posterolaterally with the paraoccipital process (= mastoid region) of the petrosal, and anterolaterally with the tympanohyal. Its posterior margin forms the ventral portion of the anterior wall of the jugular foramen and the medial wall of the stylohyal fossa (Fig. 2a).

The entotympanic MLP 3–136 of *G. robustum* is broadly similar to that of *Mylodon* described by Patterson et al. (1992) in relation to its anteroposterior length (from the pterygoid to the paracondylar process) and in the marked division of the two plates by the carotid sulcus. It also accords with the entotympanic of *G. robustum* depicted in detail by Guth (1961), but differs from the entotympanic described by Owen (1842) and van der Klaauw (1931), who attribute a shorter and blockier entotympanic to this species. These differences were treated by Patterson et al. (1992), where two different scenarios were proposed: the misidentification of the specimen studied by Guth (1961) (a specimen of *Mylodon* misidentified and assigned to *Glossotherium*) or the high variation of this structure in *Glossotherium*. Given the unambiguous attribution of this specimen to the species *G. robustum* (see Supplementary Information S2), the latter should be considered the more reliable hypothesis.

Petrosal and middle ear cavity Due to the lack of ecto- and entotympanic in MACN Pv 13553, the petrosal is visible in ventral and lateral views (Fig. 1). In ventral view the promontorium is dominant, with its lateral surface rounded and with straight margins anteriorly and ventrally, converging at almost a right angle. A wide exposure of the petrosal in ventral view is a characteristic of the lestodontine sloths, and is occasionally present also in the genus *Paramylodon* (Gaudin 1995: char. 12), where the entotympanic is strongly reduced in size.

In lateral view, the most ventral aperture on the petrosal corresponds to the aperture of the cochlear fossula (with the fenestra cochleae recessed inside; see Wible 2010; Gaudin 2011), which is clearly exposed laterally, and faces also ventrally and posteriorly (Fig. 1). It is characterized by the presence of a well-developed groove extending medially from its margin, which is a synapomorphy of the Mylodontinae (Gaudin 1995: char. 47). In the posterodistal margin of this opening, a strong bony shelf constitutes the roof of the postpromontorial tympanic sinus, a space furtherly limited posteriorly by the tympanohyal and medially by the entotympanic (Figs. 1 and 3). This shelf extends laterally and anteriorly into an evenly strong crista interfenestralis, which separates the fenestra cochleae from the fenestra vestibuli (stapedial ratio: 1.35; Figs. 1 and 3). This latter, ovate opening faces laterally, but also slightly anteriorly and dorsally. Posterior to this aperture, there is a deep fossa for the stapedius muscle, separated from the facial sulcus by a minute ridge. The deep groove for the facial nerve (VII) runs dorsally and laterally to the fenestra vestibuli and extends from the anteriormost part of the petrosal (where it emerges from the secondary facial foramen), to the base of the tympanohyal posteriorly. It is bordered laterally by a strong crista parotica of the petrosal, which is the main element on the lateral edge of the promontorium (Figs. 1 and 3). The anteroventral process of the tegmen tympani (= processus crista facialis in Patterson et al. 1992; Gaudin 1995, 2004; Wible and Gaudin 2004) is extremely reduced. It consists in a tiny concave platform, roughly triangular in shape, extending anteriorly, laterally, and ventrally (Figs. 1

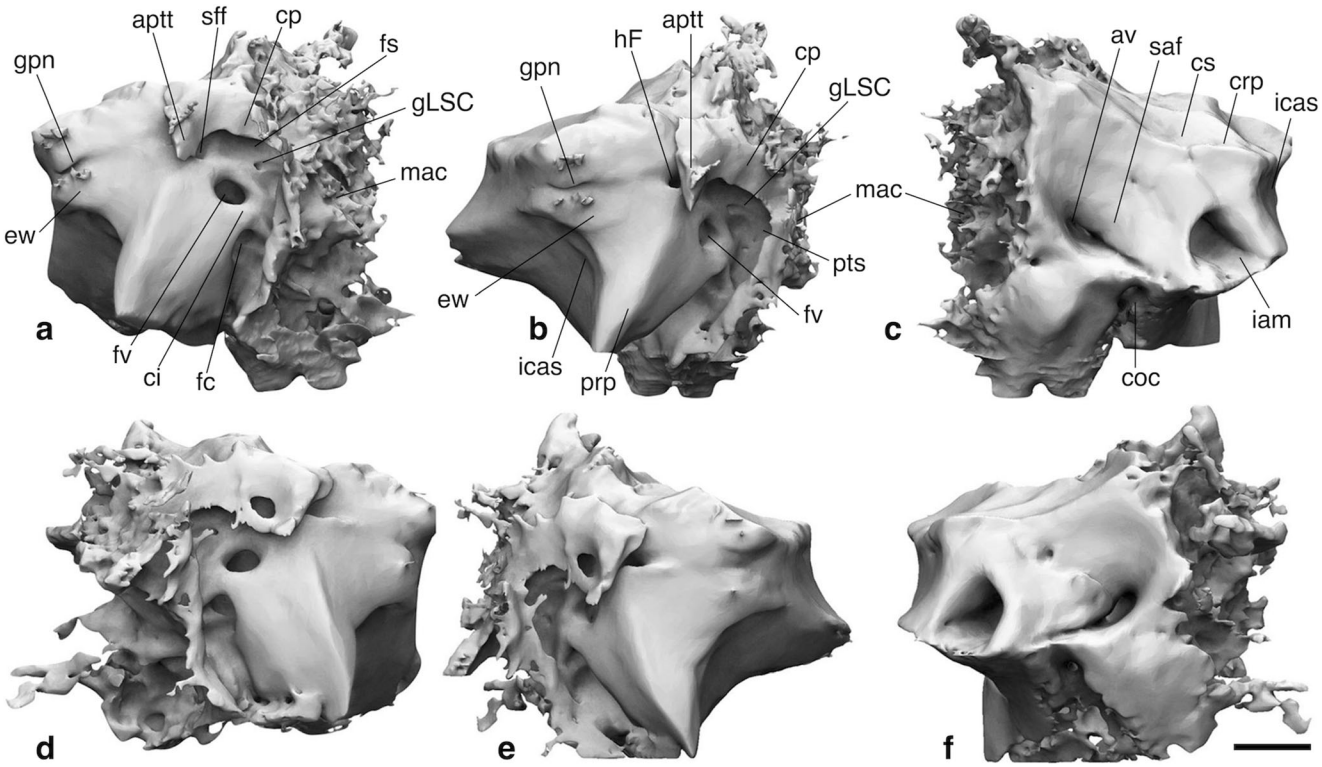

Fig. 3 Left (**a–c**) and right (**d–f**) petrosals of *Glossotherium robustum* (MACN Pv 13553), in oblique frontolateral (**a, d**), frontal (**b, e**), and posteromedial (**c, f**) views. Abbreviations: aptt, anteroventral process of the tegmen tympani; av, aqueductus vestibuli; ci, crista interfenestralis; coc, cochlear canaliculus; cp, crista parotica; crp, crista petrosa; cs, cerebral surface; ew, epitympanic wing of petrosal; fc, fenestra cochleae (= fenestra rotunda); fs, facial sulcus; fv, fenestra vestibuli (= fenestra ovalis); gLSC, groove for the lateral semicircular canal; gpn, sulcus for the greater petrosal nerve; hF, hiatus Fallopii; iam, internal acoustic meatus; icas, internal carotid artery sulcus; mac, mastoid air cells; prp, promontorium of petrosal; pts, post-tympanic sinus; saf, subarcuate fossa; sff, secondary facial foramen. Scale bar equals 1 cm

and 3). This process is separated from the promontorium by a narrow groove, which probably accommodated the greater petrosal nerve, a branch of the cranial nerve VII emerging from the hiatus Fallopii and continuing anteriorly across the ventral surface of the pterygoid (Figs. 1 and 3; Wible 2010; Gaudin 2011). Dorsal and lateral to the crista parotica, a large epitympanic recess—the epitympanic sinus of megatherioid sloths (Gaudin 2004) is not present—extends upwards into the squamosal bone (Fig. 1). This conformation is common among the Mylodontidae and is shared with some other xenarthrans (e.g., the dasypodine and tolypeutine armadillos; Patterson et al. 1989; Gaudin 1995, 2004; Wible 2010). The fossa incudis is located in the posteromedial corner of the epitympanic recess.

Additional frontal and posteromedial views of the petrosals have been obtained through the 3D digital reconstruction and image processing of MACN Pv 13553 (Fig. 3). In frontal view, the promontorium of the petrosal appears to be directed ventrally and medially (Fig. 3b, e). On the internal side, the promontorium shows a marked curvature at the level of the sulcus for the internal carotid artery. This sulcus is limited dorsally by a prominent bulge, known as the epitympanic wing (Fig. 3b, e). The latter, in turn, is grooved by the sulcus for the greater petrosal nerve, exposed in frontal view (Fig. 3b, e). The dorsal surface of the petrosal (i.e., the cerebellar surface) is essentially flat and slightly inclined anteriorly and medially (Fig. 3c, f). In posteromedial view, the two main apertures are, anteriorly, the internal acoustic meatus, and posteriorly the aqueductus vestibuli (Fig. 3c, f). The internal acoustic meatus of *Glossotherium* is a deep and undivided canal that runs posteromedially. This pattern is common in sloths, with the only exceptions represented by *Hapalops* and the extant genera *Bradypus* and *Choloepus* (Gaudin 1995: chars. 48 and 49). In *G. robustum* MACN Pv 13553, the common floor for the internal acoustic meatus and the aqueductus vestibuli is ventrally and medially extended and, at the level of the aqueductus vestibuli, it serves as the roof for the cochlear canaliculus, whose section is circular in shape (Fig. 3c, f). In frontal and posteromedial views, we observed marked asymmetries between the left (Fig. 3a–c) and right (Fig. 3d–f) petrosals. Some of these differences can be easily attributed to breakage or differential preservation (e.g., the breakage at the level of the crista parotica or the exposure of the lateral semicircular canal, Fig. 3a–b, d–e). Others differences, like the different widths of the sulci for the greater petrosal nerve (Fig. 3b, e) and the differing shapes of the internal acoustic meatus and the aqueductus vestibuli (Fig. 3c, f), correspond to real variation between the two sides.

The internal acoustic meatus is rounded on the left petrosal (Fig. 3c), whereas it is more quadrangular on the right side (Fig. 3f). Also, the bony wall between the internal acoustic meatus and the aqueductus vestibuli, marking the rim of the subarcuate fossa, also displays some differences. It is smooth on the left petrosal (Fig. 3c), whereas it is marked by protuberances and deep pits on the right (Fig. 3f).

Tympanohyal and stylohyal fossa The tympanohyal of *G. robustum* is typically sloth-like: narrow at its base and enlarging distally into a circular head (Patterson et al. 1992; Gaudin 1995: char. 52). It is directed ventrally and slightly posteriorly, and its distal surface forms a major portion of the stylohyal fossa (Fig. 1). This fossa is an articular surface for the stylohyal, common to all sloths excluding the extant genus *Bradypus* (Patterson et al. 1992; Gaudin 1995, 2004, 2011). The other bones participating in the stylohyal fossa are the entotympanic anteromedially, the paracondylar process of the exoccipital posteromedially, and the mastoid portion of the petrosal posterolaterally. The stylohyal fossa is circular in shape and ventrolaterally oriented (Figs. 1 and 2). This slight tilt is characteristic of the extant two-toed sloth *Choloepus*, but also *Planops*, *Hapalops*, and the majority of mylodontids (Gaudin 1995: char. 56).

Exoccipital and petrosal (mastoid region) The paracondylar process of the exoccipital forms part of the stylohyal fossa laterally (as noted above) and the posterolateral wall of the jugular foramen on its medial side. It is ventrally and anteriorly extended, and continuous posteriorly with the exoccipital crest (Fig. 1a). More posteriorly, the exoccipital crest enlarges towards the occipital condyle, which it approaches but does not contact.

The exoccipital crest is bounded anterolaterally by the mastoid exposure of the petrosal, which continues ventrally into the stylohyal fossa. It has the same anteroventral inclination as the exoccipital crest, but its surface is somewhat depressed, forming the so-called mastoid depression or digastric fossa (Gaudin 1995: char 32; Gaudin and Wible 2006). At the ventrolateral margin of the mastoid depression is the so-called "mastoid process" (Patterson et al. 1992), which, like most mylodontines, is a low, anteroposteriorly broad process with a semicircular ventral margin. Based on a juvenile specimen of *G. tropicorum* (ROM 12673), the "mastoid process" is comprised largely of the paroccipital process of the petrosal, though the posttympanic process of the squamosal appears to make a small anterodorsal contribution. Two well-marked foramina are near to the paraoccipital process: the ventral opening for the occipital artery (= mastoid foramen in Patterson et al. 1992) and the stylomastoid foramen. The two foramina are connected by a very weak groove (Figs. 1 and 2), a feature also present in *Pleurolestodon*, *Paramylodon*, *Lestodon*, and *Thinobadistes* (Gaudin 1995: char. 59, 2004). Therefore, the ventral opening for the occipital artery lies within the mastoid region of the petrosal, whereas the stylomastoid foramen lies between the paraoccipital process of the petrosal (laterally and dorsally), the tympanohyal (medially), and the squamosal (anteriorly). The stylomastoid foramen, accommodating the facial nerve (cranial nerve VII), lies at the terminus of a canal that is continuous with the facial sulcus of the petrosal (Figs. 1 and 2). Leaving the middle ear cavity, this canal is ventrolaterally directed, a typical feature in the Mylodontidae (Gaudin 1995: char. 58, 2004). The stylomastoid foramen itself is situated anterior to the stylohyal fossa, a recurrent character in the Mylodontinae (Gaudin 1995: char. 57, 2004).

Squamosal The squamosal-petrosal suture is not visible because of the complete fusion between these bones. However, its putative position is traced in Fig. 1a (dashed line), on the basis of the aforementioned juvenile specimen of *G. tropicorum* (ROM 12673). Both zygomatic processes of the squamosal are missing in MACN Pv 13553 (Supplementary Information S1), but visible in MLP 3–136 (Supplementary Information S2), where they are anteriorly and laterally directed. Posteriorly, they meet the paraoccipital process of the petrosal in a marked depression on the lateral surface of the post-tympanic process of the squamosal. This depression extends ventrally to form the superficies meatus (Figs. 1 and 2).

The squamosal forms the lateral wall and roof of the large epitympanic recess, but also part of its anterior and posterior walls. This capacious cavity also extends slightly into the root of the zygoma, as in many xenarthrans (Patterson et al. 1992; Gaudin 2004, 2011).

Pterygoid In both specimens, the pterygoids are greatly inflated and separated into two portions, medial and lateral, whose division is more marked posteriorly than anteriorly (Figs. 1 and 2). As in *Mylodon*, the lateral portion of the pterygoid is inflated, its sinus partially invading the squamosal (Fig. 1a; Patterson et al. 1992). By contrast, the medial portion of the pterygoid is more globose and less anteroposteriorly enlarged than the lateral region. In this portion, the inflation also extends partially into the basisphenoid and forms the anterior and medial walls of the carotid foramen, whereas the lateral and posterior walls of this opening, as mentioned above, are formed by the entotympanic (Figs. 1 and 2). As in the other representatives of the Mylodontinae, the carotid foramen is fully exposed in ventral view (Gaudin 1995: char. 15, 2004).

Basisphenoid and basioccipital The boundary between the basisphenoid and the basioccipital, which together constitute the floor of the basicranium, cannot be described in either specimen due to the complete fusion of their sutural contacts (Fig. 1a). However, the basisphenoid is normally in contact with the pterygoid and is involved in the formation of the

carotid foramen in sloths, whereas the basioccipital, which typically extends from the posteriormost edge of the carotid foramen to the anteroventral rim of the foramen magnum (Patterson et al. 1992; Gaudin 2011), is directly involved in the formation of the jugular and the hypoglossal foramina (Figs. 1a and 2a). As noted previously, the jugular foramen is limited anteriorly by the entotympanic and posterolaterally by the exoccipital. The basioccipital surrounds it posteromedially.

Bony labyrinth (inner ear)

Description and comparison The inner ear of *G. robustum* MACN Pv 13553 appears very small relative to skull size (Fig. 4), in this sense more closely resembling the labyrinth of *Megatherium*, the only inner ear of a fossil xenarthran available for comparison (Billet et al. 2013: Fig. 1), than those of the extant sloths (Billet et al. 2012: Fig. 1). This was to be expected, given the allometric relationship between the inner ear and petrosal and the skull (Billet et al. 2015b), as well as the allometry between body mass and the size of the inner ear and petrosal (Jones and Spells 1963; Muller 1999; Spoor et al. 2007). The visualization of the inner ear within the surrounding posterior cranium (Fig. 4) also shows that the lateral semicircular canal is very obliquely oriented relative to the horizontal plane, as observed for fossil sloths and extant armadillos (Coutier et al. 2017).

As observed for *Megatherium* (Billet et al. 2013) and reported for *Lestodon* and *Catonyx* in a published abstract (Varela et al. 2016), the semicircular canals in *Glossotherium* are thin (i.e., with a small cross-sectional diameter) with a large radius of curvature with respect to the vestibular region (Figs. 4 and 5), whereas they are thicker with a smaller radius of curvature in extant sloths (Billet et al. 2012, 2013, 2015a). Among xenarthrans, semicircular canals with a reduced radius of curvature are only observed in extant sloths and in the pink fairy armadillos (i.e., *Chlamyphorus*; Billet et al. 2015a: char. 10). However, there are some remarkable differences between *Glossotherium* and other sloths. For example, the angle between the anterior and posterior semicircular canals is acute in *Glossotherium* (78.2°), but is obtuse (> 90°) in all the extant sloths and in *Megatherium.* Among the other xenarthrans here considered, the latter condition is only observed in *Chaetophractus* (Billet et al. 2015a: char. 12).

The two extinct sloths also differ in the arrangement of the posterior root and arch of the lateral semicircular canal. In *Glossotherium* (Fig. 5), the posterior root of the lateral semicircular canal lies at the level of the ampullar entrance of the posterior semicircular canal, whereas in *Megatherium* it is situated much further dorsally (Billet et al. 2015a: char. 1). The latter condition is variably observed in *Bradypus* and is characteristic of the cingulate genus *Dasypus*, whereas the former condition is shared by all the other xenarthrans observed. The lateral semicircular canal of *Glossotherium*

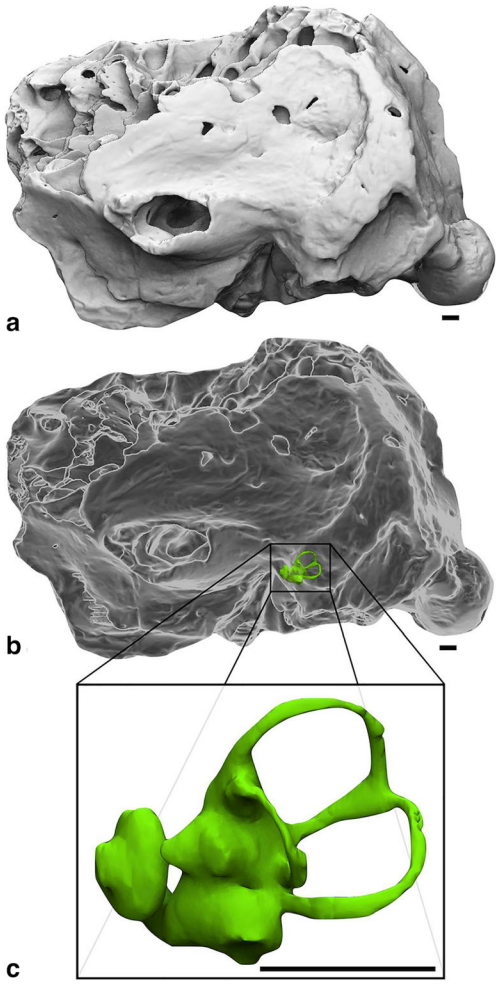

Fig. 4 Three-dimensional reconstructions of the neurocranium and the bony labyrinth of *Glossotherium robustum* (MACN Pv 13553). (**a, b**) neurocranium in lateral view (**b**, transparency, showing the bony labyrinth of the inner ear in opaque green) (anterior towards left); (**c**) close-up of the left bony labyrinth of the inner ear (anterior towards left, dorsal towards top). Scale bar equals 1 cm

(Fig. 5) presents only a weak torsion (Billet et al. 2015a: char. 4), as observed in almost all the xenarthrans with the exception of *Megatherium* and *D. novemcintus,* in which the torsion is more pronounced (Billet et al. 2015a). The *G. robustum* specimen MACN Pv 13553 also possesses an entrance into the posterior limb of the lateral semicircular canal from the posterior ampulla, a condition only observed in the pygmy anteater *Cyclopes* and *Chlamyphorus* (Billet et al. 2015a: char. 5). The lack of the bulge in the utricular region of *Glossotherium* (Fig. 5) is another marked difference with *Megatherium*. This bulge is also variably developed in *Choloepus,* but is absent in *Bradypus* and all other xenarthrans (Billet et al. 2015a: char. 16).

A feature that could link all the sloths considered here is the absence of the secondary bony (basilar) lamina sulcus on the cochlear endocast (Fig. 5), a condition that is also observed in *Chlamyphorus* (Billet et al. 2015a: char. 11).

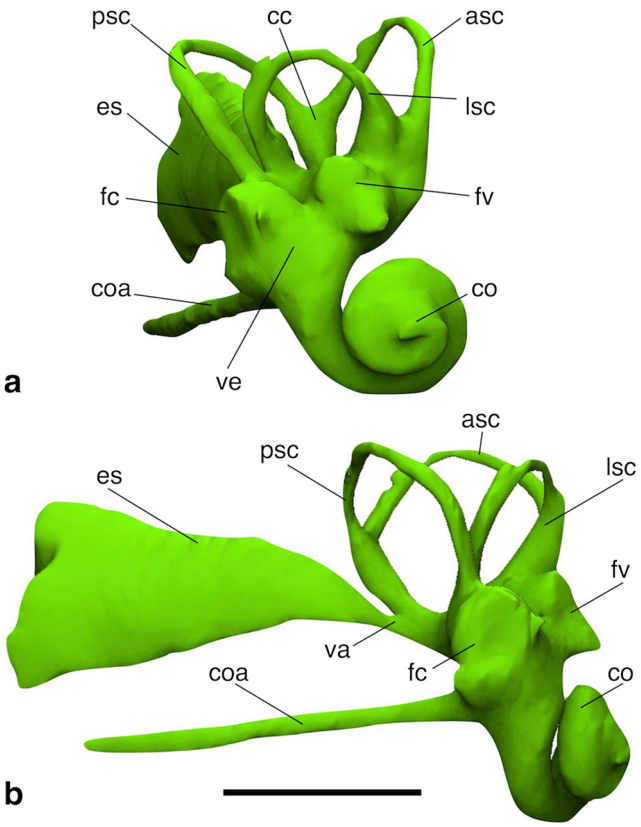

Fig. 5 Three-dimensional reconstruction of the right inner ear of *Glossotherium robustum* (MACN Pv 13553) in (**a**) frontolateral and (**b**) ventrolateral views. Abbreviations: **asc**, anterior semicircular canal; **cc**, crus commune; **coa**, cochlear aqueduct; **co**, cochlea; **es**, endolymphatic sac; **fc**, fenestra cochleae (= fenestra rotunda); **fv**, fenestra vestibuli (= fenestra ovalis); **lsc**, lateral semicircular canal; **psc**, posterior semicircular canal; **va**, vestibular aqueduct; **ve**, vestibulum. Scale bar equals 1 cm

Plesiomorphic features shared by all the sloths considered here are the presence of a small fenestra vestibuli (Billet et al. 2015a: char. 3), and the orientation of the vestibular aqueduct and cochlear canaliculus, which are subparallel or slightly oblique relative to the crus commune (Fig. 5; Billet et al. 2015a: char. 9). These conditions are invariably present in pilosans, whereas derived states of these features are observed among the armadillos (Billet et al. 2015a).

Finally, a labyrinthine feature linking *Glossotherium* with the giant anteater *Myrmecophaga* involves the cochlear canal, which is particularly short relative to inner ear size. Both taxa also have fewer than two cochlear coils (Fig. 5; Billet et al. 2015a: char. 7).

Morphometric geometric results The overall shape similarity between the bony labyrinth of the genus *Glossotherium* and those of anteaters is further reinforced by morphometric data analysis, conducted on the 80 semilandmark dataset. The PCA based on the entire bony labyrinth (Fig. 6) reveals that *Glossotherium* most closely resembles the extant anteaters, and to a lesser degree *Megatherium* and the armadillos. The similarity of the bony labyrinth of *Glossotherium* to those of extant anteaters is recovered on both PC1 (positive values) and PC2 (negatives values), and is correlated with an enlargement of the semicircular canals, a smaller cochlea, and a more acute angle between the anterior and the posterior semicircular canals (PC1, positive values), as well as a longer crus commune and a reduced separation between the anterior and posterior semicircular canals dorsal to the crus commune (PC2, negative values) (Fig. 6a). On PC3, armadillos and anteaters are not clearly separated, and *Glossotherium* is again closely associated with the anteaters and, to a lesser degree, with the dasypodid armadillos and *Megatherium* (Fig. 6b).

A second PCA was performed exclusively on the semicircular canal semilandmark subset (Fig. 7) and showed results very similar to the first PCA (Fig. 6), with *Glossotherium* even closer to *Myrmecophaga* and *Tamandua* (the lesser or collared anteater) than any other xenarthran. The genera *Myrmecophaga*, *Tamandua*, and *Glossotherium* fall into the higher values of PC1, associated with larger semicircular canals, a less inclined crus commune and a reduced angle between the anterior and posterior semicircular canals; and, into the lower values of PC2, corresponding, in its most extreme values (e.g., *Cyclopes*), to a dorsoventrally elongated posterior semicircular canal smaller than the rounded anterior semicircular canal, and a narrower crus commune (Fig. 7a). As in the former analysis (Fig. 6b), the PC3 does not reliably separate any group, and the genus *Glossotherium* is more closely associated with the anteaters, the euphractine armadillos and *Megatherium* than any other xenarthran (Fig. 7b).

In the same way, we performed a third PCA, this time considering only the cochlear semilandmark data set (Fig. 8). In this PCA, *Glossotherium* sits close to *Megatherium*, *Myrmecophaga*, and the euphractine armadillos and falls into higher values of PC1 and slightly negative values of PC2 (Fig. 8a), which correspond to a low spired and asymmetrically-convoluted cochlea. Along PC3 (Fig. 8b) *Glossotherium* falls in the middle of the shape range, close to anteaters, euphractine armadillos and two-toed sloths.

The same PCAs were also conducted with the shape data corrected for allometry, using either body mass (Supplementary Information S4) or centroid size (Supplementary Information S5) as estimators of size, which respectively explain the 10.25 and 8.63% of the labyrinthine shape variation. Given the low influence of allometry (see Billet et al. 2015a), these PCAs are very similar to the previous ones (Figs. 6–8) and the results are available in the supplementary material (Supplementary Information S4–S5). The allometric shape vector (ASV) and partial least square (PLS) analyses are also similar to those of Billet et al. (2015a).

The ASV analyses enable us to observe the transformations of the whole labyrinth that are related to allometry (Supplementary Information S6–S7). Regarding the two extinct sloths considered, *Megatherium* tends to be separated

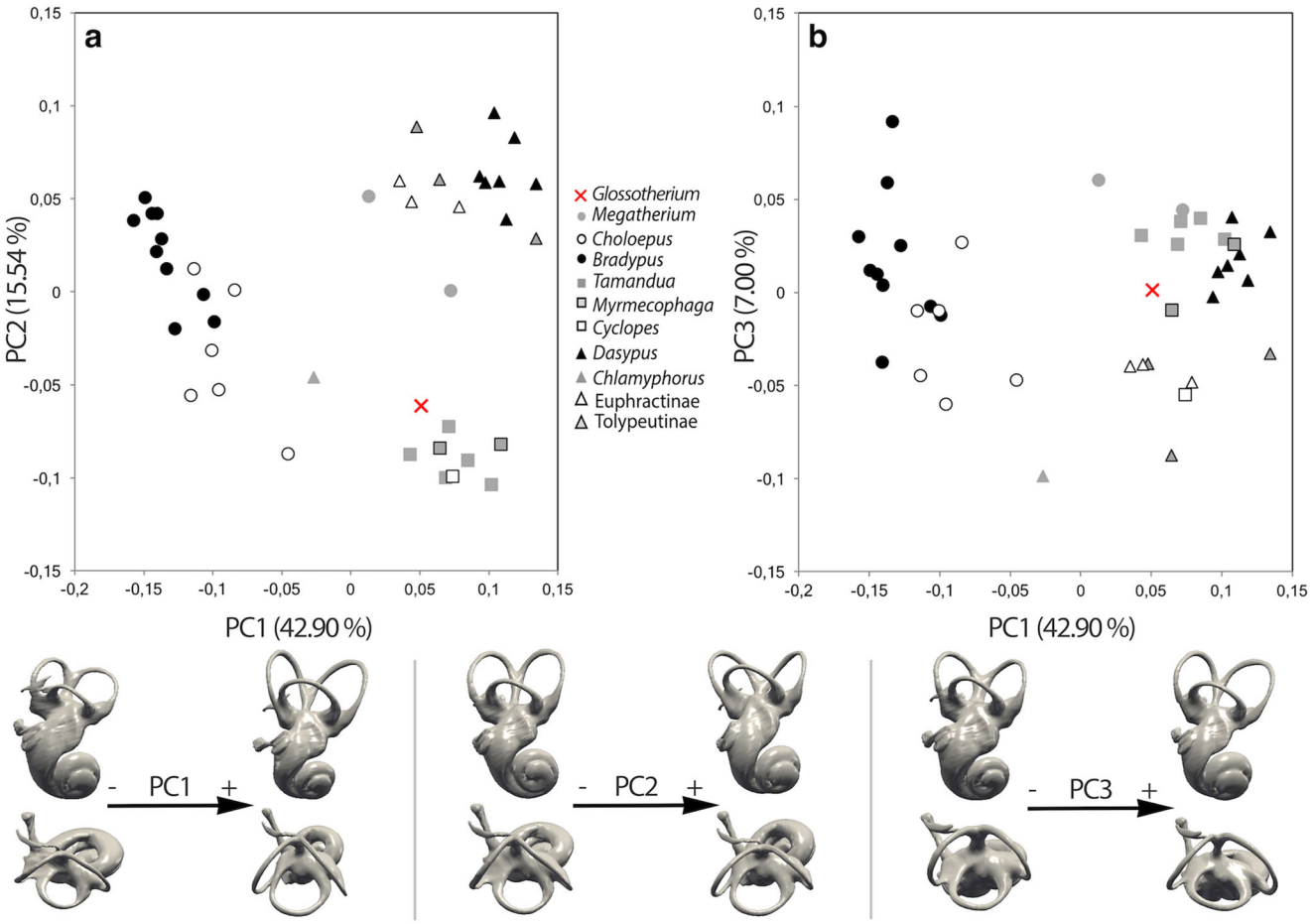

Fig. 6 Principal component analysis performed on the total set of 80 semilandmarks, showing the shape differentiation of the bony labyrinth among extant xenarthrans, as well as the two extinct sloths *Glossotherium* and *Megatherium*. **a** Principal components 1 and 2 and **b** principal components 1 and 3. At the bottom: associated patterns of morphological transformation on the first 3 axes (65.44% of the among-group variance)

from the extant xenarthrans, a probable consequence of its extreme weight and size (Billet et al. 2015a). However, despite its large body mass (less than 30% of *Megatherium*, but around 37 times the mass of the largest extant xenarthran), *Glossotherium* sits among the higher values for the allometric shape vectors that are typical of the extant anteaters (Supplementary Information S6–S7).

Covariation between the semicircular canals and the cochlea was also examined by performing a PLS analysis (Supplementary Information S8). On the first singular warp (SW1; Supplementary Information S8), we observe the same association of cochlear and semicircular canal features described by Billet et al. (2015a: Fig. 7a): small semicircular canals (i.e., with a small radius of curvature) with an obtuse angle between the anterior and the posterior canals are associated with a long and convoluted cochlea, oriented obliquely relative to the lateral semicircular canal. *Glossotherium* is close again to the anteaters, the euphractine armadillos, and *Megatherium*. On the second singular warp (SW2; Supplementary Information S8) the short crus commune and the small semicircular canals with divergent anterior and posterior canals, are associated with a cochlea that has a larger diameter and a taller spire. *Glossotherium* is recovered near the boundary between the extant sloth *Choloepus* and anteaters in this analysis.

Discussion

External anatomy of the basicranium and petrosal bone in *G. robustum* The description of well-preserved specimens of *G. robustum* allowed a detailed characterization of the ear region, showing different aspects of variation, at both intraspecific and intraindividual levels. The entotympanic (Fig. 2) strongly contrasts with those described by Owen (1842) and van der Klaauw (1931), and instead resembles those depicted by Guth (1961) for the same taxon. This reinforces the hypothesis of Patterson et al. (1992), who suggested the existence of marked intraspecific variation of the entotympanic in *G. robustum*.

CT-scanning techniques also revealed the "hidden" views of the petrosals, namely the frontal and posteromedial views,

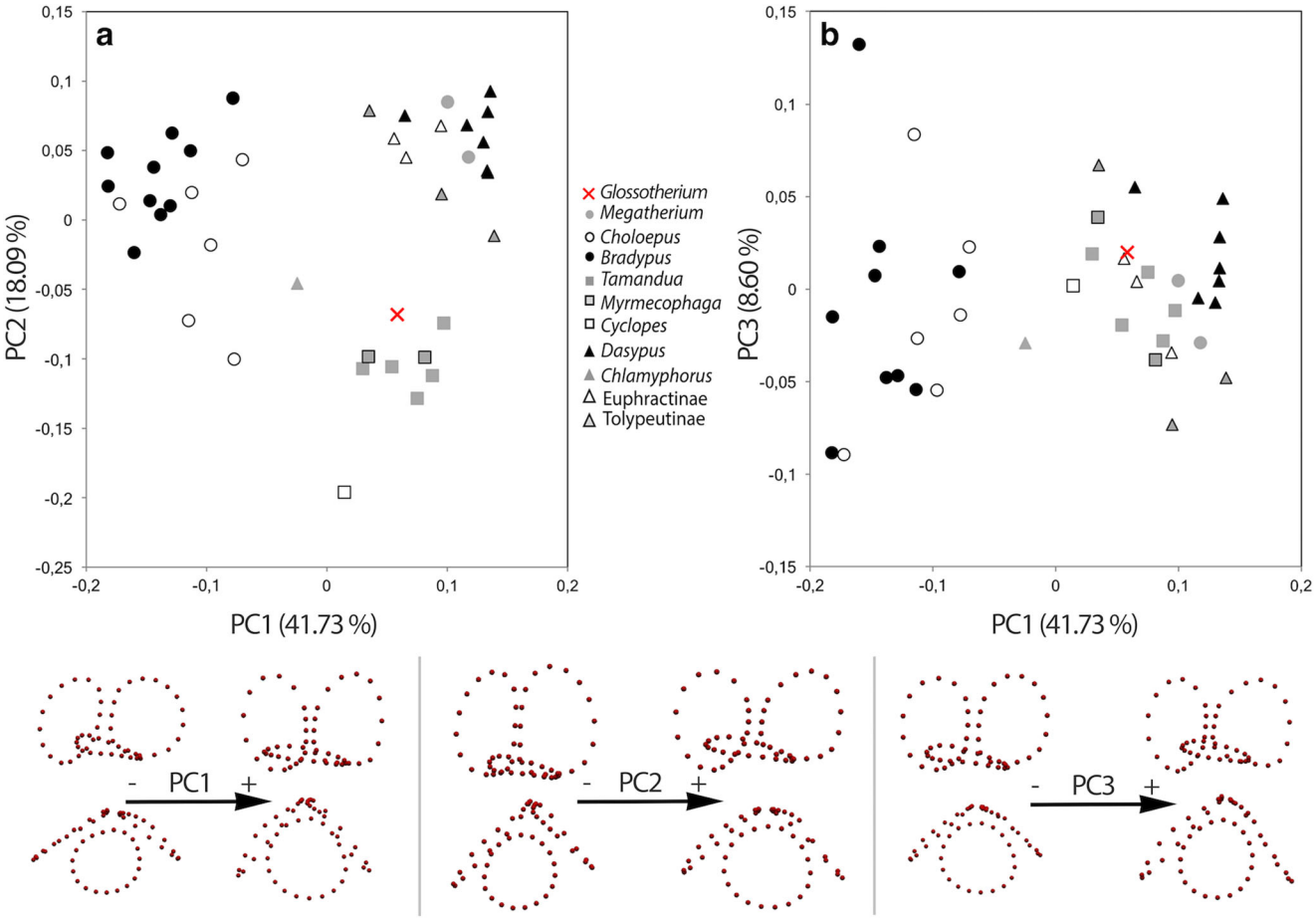

Fig. 7 Principal component analysis performed on a subset of 60 semilandmarks, showing the shape differentiation of semicircular canals among extant xenarthrans, as well as the two extinct sloths *Glossotherium* and *Megatherium*. **a** Principal components 1 and 2 and **b** principal components 1 and 3. At the bottom: associated patterns of morphological transformation on the first 3 axes (68.42% of the among-group variance)

which exhibit bilateral variation (Fig. 3). These observations are in accordance with those of Danilo et al. (2015), who observed strong variation between the left and right petrosals of a large sample of the extant perissodactyl *Equus caballus przewalskii*. This variation appeared to be mostly related to the form of the internal acoustic meatus and the subarcuate fossa, which exhibited different sizes and differing degrees of elongation and depth (Danilo et al. 2015). In contrast, Danilo et al. (2015) observed less variation at the level of the bony labyrinths, which showed little bilateral asymmetry. Our data on the frontal and posteromedial views of the petrosal of *G. robustum* specimen MACN Pv 13553 shows marked asymmetry at the level of the openings for the greater petrosal nerve, the internal acoustic meatus and the aqueductus vestibuli (Fig. 3).

Internal anatomy: the bony labyrinth of the inner ear Billet et al. (2015a) discussed in detail both the weak influence of allometry and the strong imprint of phylogeny in their sample of bony labyrinths among xenarthrans. The inclusion of the genus *Glossotherium* in the present dataset allowed us to extend Billet et al.'s (2015a) observations to a sample now including a member of the diverse extinct sloth family Mylodontidae. Regarding allometry, even if the influence of size is rather low in the new dataset (accounting for 10.25 and 8.63% of labyrinthine shape variation using body mass and centroid size corrections, respectively), it is slightly higher than the values for the previous dataset (9.94 and 7.64% respectively; Billet et al. 2015a). An increase in allometric effect was also observed by removing *Megatherium* from the extant dataset (Billet et al. 2015a). The stronger allometric effect with the inclusion of *Glossotherium* suggests that further integration of other large to medium-sized extinct xenarthrans will enable more reliable evaluation of the effect of allometry.

In contrast, the imprint of phylogeny on labyrinthine shape is remarkable in the previous dataset, with the exceptions of the genera *Chlamyphorus* and *Megatherium* (Billet et al. 2015a). This scenario is further complicated with the inclusion of *Glossotherium*, since it is strongly associated with extant anteaters (and to a lesser degree *Megatherium* and the extant armadillos) in the first three axes of all PCAs in our results.

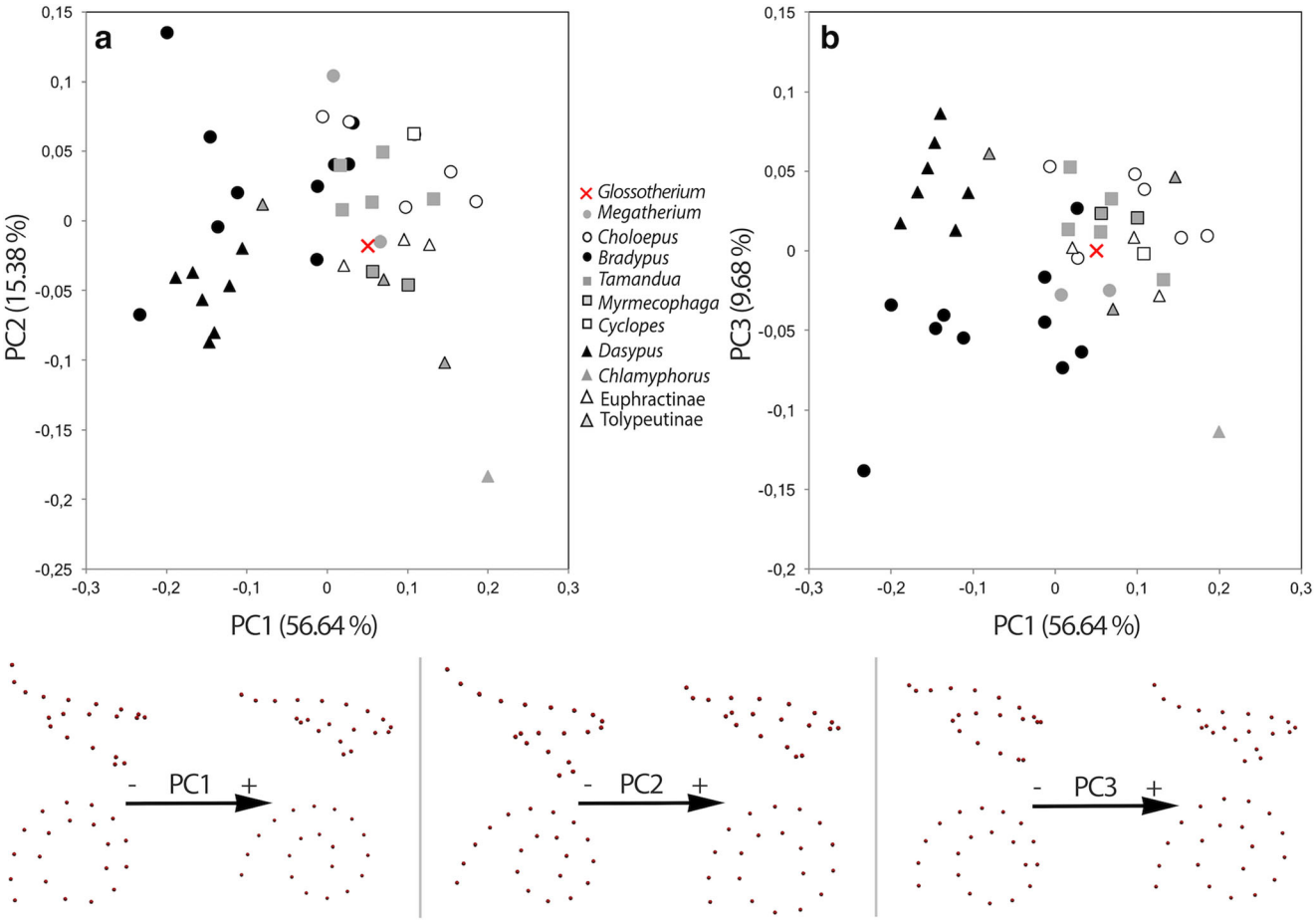

Fig. 8 Principal component analysis performed on a subset of 20 semilandmarks, showing the shape differentiation of the cochlea among extant xenarthrans, as well as the two extinct sloths *Glossotherium* and *Megatherium*. **a** Principal components 1 and 2 and **b** Principal components 1 and 3. At the bottom: associated patterns of morphological transformation on the first 3 axes (81.70% of the among-group variance)

This suggests that functional factors might also be responsible for the observed distribution. For this reason, some of the methods linking inner ear morphology with particular functional attributes were tentatively applied to *Glossotherium* and critically reviewed.

Functional considerations for the semicircular canals As already noted by Billet et al. (2015a), most of the morphological transformations of the xenarthran bony labyrinth are ascribable to changes in the configuration of the semicircular canals (Figs. 6 and 7). The semicircular canals, together with the utricle, help in detecting the angular acceleration and deceleration of the head, stabilizing the gaze during locomotion, and aid in the coordination of body movements (e.g., Spoor et al. 2007; Sipla and Spoor 2008; Silcox et al. 2009; David et al. 2010; Ekdale 2016).

Spoor et al. (2007) assigned six agility categories to a mammalian sample, from extra slow (e.g., extant sloths) to fast (e.g., bats), and observed that agile mammals have significantly larger semicircular canals (i.e., with a larger radius of curvature) relative to body mass than those that move more slowly. In the graph depicted in Fig. 9, modified after Spoor et al. (2007) and Billet et al. (2013), *Glossotherium* falls in the top-right corner, close to *Megatherium* and modern mammals of similar size, most of which were classified as medium-slow animals by Spoor et al. (2007). Elephants are the extant mammals that best approximate the relative size of the semicircular canals and body mass of *Megatherium* (Billet et al. 2013), whereas for *Glossotherium* the hippopotamus is the closest taxon (see the gray circles in Fig. 9 close to *Megatherium* and *Glossotherium,* respectively). However, this association is probably much more strongly influenced by the correlation between semicircular canal length and body size than it is by the (weaker) correlation with agility (Malinzak et al., 2012). In fact, graphical comparisons can only be made at a given body mass (Billet et al. 2013; Ruf et al. 2016), and the method of Spoor et al. (2007) and the predictive equations of Silcox et al. (2009) are difficult to apply for extremely small-sized and large-sized mammals (Billet et al. 2013). Even more so, a direct comparison of the extinct sloths with the extremely

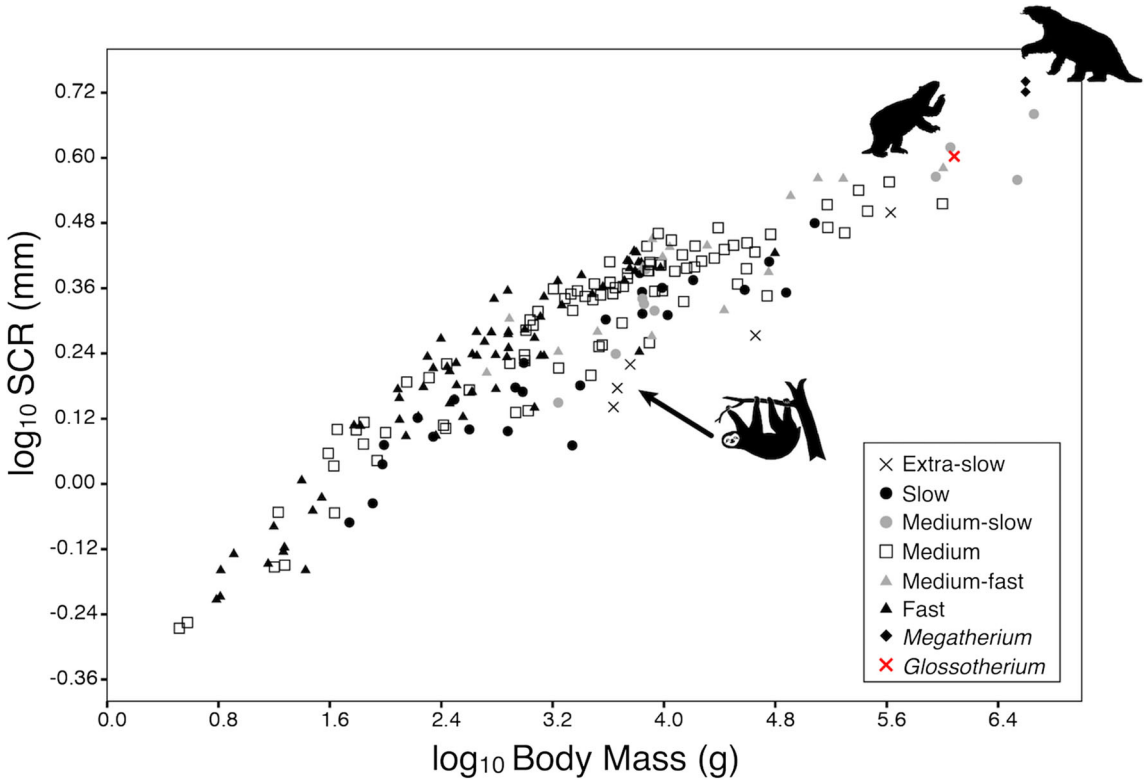

Fig. 9 Double logarithmic plot of average semicircular canal radius (SCR) against body mass for 210 mammals, after Spoor et al. (2007) and Billet et al. (2013), showing the graphical relationship among semicircular canal sizes, body mass and agility

slow extant sloths cannot be undertaken at the moment, due to the striking difference in body size (Billet et al. 2013). However, what is evident in the graph in Fig. 9 is that *Glossotherium*, like *Megatherium* but in contrast to extant sloths, has semicircular canals of similar or perhaps slightly greater length, relative to those of similar-sized mammals.

The orientation of the semicircular canals relative to one another has been linked to the sensitivity of the equilibrium system (Malinzak et al. 2012; Berlin et al. 2013). Malinzak et al. (2012) proposed that the closer the angles among the semicircular canal planes are to orthogonality (90°), the higher the sensitivity to head rotations (Malinzak et al. 2012; Berlin et al. 2013). The bony labyrinth of *Glossotherium* shows a pronounced deviation from orthogonality: following the protocol of Berlin et al. (2013) the 90_{var} is 12.28 ($\log_{10}90_{var}$ = 1.09), which is close to the lowest values for average sensitivity in the dataset of Berlin et al. (2013). These values, in turn, are associated by Berlin et al. (2013) with fossorial habits. The average 90_{var} value for the fossorial taxa in that sample (mean = 11.0°; st. dev. = 3.2°) is twice that of non-fossorial taxa (mean = 5.5°; st. dev. = 1.8°). Despite the fact that large Pleistocene "burrows" in the Pampean region have repeatedly been attributed to the activity of mylodontid sloths (e.g., Zárate et al. 1998; Vizcaíno et al. 2001; Blanco and Rinderknecht 2012), *G. robustum* was almost certainly not an obligate fossorial taxon like those included in Berlin et al.'s (2013) dataset. Moreover, among extant xenarthrans, the $\log_{10}90_{var}$ calculated for *G. robustum* (1.09), is closer to the range calculated for the non-fossorial *Tamandua tetradactyla* (1.42 to 2.63) and *Bradypus variegatus* (1.73–3.08) than those calculated for *Dasypus novemcintus* (2.25–2.49) (Billet et al. 2012; Ruf et al. 2016). Among the extant xenarthrans for which this value was calculated in Ruf et al. (2016), *Dasypus novemcintus* is the only taxon that displays burrowing habits (Gaudin and Biewener 1992), and it is, indeed, the most distant data point from *Glossotherium*. This data shows that burrowers do not necessarily display lower degrees of canal orthogonality and confirm that, to date, "it is not functionally clear why lower degrees of canal orthogonality would be associated with a burrowing lifestyle" (Berlin et al. 2013: p. 14). Ruf et al. (2016) also stressed the fact that the correlation coefficients of the regressions in Berlin et al. (2013) are quite modest, and that both Malinzak et al. (2012) and Berlin et al. (2013) do not take into account non-negligible intraspecific variation.

Recent studies (e.g., Billet et al. 2012; Perier et al. 2016; Ruf et al. 2016) have been considering the intraspecific variation of the bony labyrinth as a useful tool to properly characterize distinct morphologies, but also as an important parameter for inferring function. Billet et al. (2012) noticed that the extant sloths show a surprisingly high degree of intraspecific variation, particularly in their semicircular canals, compared with

other mammals. This higher amount of intraspecific variation of the bony labyrinth was related with a possible relaxation of the selective pressure on its morphology, as a consequence of the reduced functional demand for rapid postural adjustments (Billet et al. 2012). This idea was reinforced by Perier et al. (2016), who concluded that the bony labyrinths of slow-moving primates show higher amounts of intraspecific variation than the fast-moving ones, though to a much lesser extent than in extant sloths. In other words, the slower an animal is, the more the bony labyrinth may vary intraspecifically (Perier et al. 2016). The latter authors, while not necessarily invalidating the results obtained by studies that include the radius or the orthogonality of the semicircular canals (e.g., Spoor et al. 2007; Malinzak et al. 2012), explicitly warn against the interpretation of measurements based on one or a few individuals per species (Perier et al. 2016).

At present, we can observe that all the extinct sloths and living armadillos and anteaters have relatively longer semicircular canals (i.e., with a larger radius of curvature; Figs. 6 and 7) than the living tree sloths. From a phylogenetic point of view, our data confirm the previous hypothesis of Billet et al. (2013) that the strange morphology of the extant sloths' semicircular canals is due to convergence, probably related with the parallel acquisition of their slow and suspensory locomotion (e.g., Gaudin 2004; Nyakatura 2012).

Functional considerations for the cochlea The cochlea is related to the sense of hearing, and many of its macroscopic features have been associated with auditory physiology (for a review see Ekdale 2016). For example, Manoussaki et al. (2008) demonstrated that the ratio of the radius of curvature in the basal cochlear spiral relative to that of the apical spiral (Radii ratio = R_{base}/R_{apex}) is correlated with low frequency hearing limits in both land and aquatic mammals. More precisely, the higher the ratio (i.e., the more asymmetric the coiling in perpendicular view), the lower the low frequency limit of hearing (Manoussaki et al. 2008). Even if this relationship is highly significant (Manoussaki et al. 2008), we observed that the procedure proposed by the authors is not straightforward. Indeed, we obtained low frequency limit values ranging from 100 to 20 Hz, depending on the measurement. Danilo et al. (2015), Ekdale and Racicot (2015) and Orliac and O'Leary (2016) reported similar repeatability issues. Despite this operational limit, it seems that low-spired cochleae in mammals have lower frequency limits, as suggested by Gosselin-Ildari (2006, in Ekdale and Rowe 2011) who found a positive correlation between the cochlear ratio (height divided by width, in lateral view) and the low frequency limit in primates. In fact, the cochlea of *Glossotherium* is one of the most low-spired and asymmetrically coiled among xenarthrans (Fig. 8). Other morphological features that support specialization for low-frequency hearing in *Glossotherium* include the overlapping turns in vestibular view and the absence of the secondary bony lamina (Ekdale and Racicot 2015). Moreover, specialized low-frequency hearing has already been proposed for *G. robustum* by Blanco and Rinderknecht (2008, 2012) on the basis of middle ear ossicle size-estimations. They suggested a low-frequency limit of 44 Hz for *G. robustum*, somewhat higher than that of modern elephants. This limit could be related to specific ecological adaptations, such as long-range communication via infrasound, and fossoriality (Blanco and Rinderknecht 2008, 2012). However, the association of *Glossotherium* with *Megatherium*, the anteaters and the euphractine armadillos, rather than with extant sloths, is consistently weaker in the cochlear dataset (Fig. 8) than in the semicircular canals dataset (Fig. 7), and more data is needed to properly evaluate if this similarity is due to functional considerations.

Conclusions

In this study, we reviewed the external features of the ear region of *Glossotherium robustum,* and provided new information on its external morphology, as well as the first data on inner ear features in this extinct sloth species. External features, highly informative from a phylogenetic point of view (Gaudin 1995, 2004), can in some parts show high levels of variation. In *G. robustum*, the entotympanic bone is highly variable at the intraspecific level, whereas the posteromedial side of the petrosal is variable even bilaterally among individuals.

Regarding the shape of the bony labyrinth in xenarthrans, the effect of phylogeny, though strong (Billet et al. 2015a), cannot explain all the observed variation. Given that allometry has a limited influence on the shape of the bony labyrinth in xenarthrans (Billet et al. 2015a), functional aspects should be taken into account when trying to explain the observed distribution. However, methods linking geometric features with functional aspects have recently been questioned, in part due to the strong phylogenetic signals (Lebrun et al. 2010; Benoit et al. 2013) and in some cases to the relatively weak correlation between subjective categories of agility and the bony labyrinth morphology (Malinzak et al. 2012). These effects are often hard to tease apart, and their interrelationships can vary among different mammalian clades. Other criticisms were expressed by David et al. (2010, 2016), who concluded that "since the degree to which the canals reflect the size and shape of the ducts inside is highly variable, such studies cannot provide the essential information for functional analyses" (David et al. 2016: p. 2). This suggests that most methods currently employed are not reliable enough for predicting functional abilities in fossil species based on the semicircular canal morphology, even if some progress is being made among extant species (David et al. 2010, 2016).

Moreover, the limited attention to intraspecific variation has been recently stressed (Perier et al. 2016; Ruf et al. 2016). This

is particularly true for extinct species, for which there is often a strong temptation to estimate habits based on the bony labyrinthine morphology of a single individual (Perier et al. 2016).

For the time being, the peculiar conformation of the semicircular canals in living sloths, coupled with their unusual locomotory mode, has not been observed in any other xenarthran, which reinforces the hypothesis that the two extant genera have undergone striking levels of convergence.

The addition of other extinct xenarthrans (especially but not exclusively limited to sloths) to the present dataset may allow clarification of the timing of these evolutionary changes.

Acknowledgments We are grateful to the FUESMEN institute (Fundación Escuela de Medicina Nuclear, Mendoza, Argentina) for access to CT-scanning facilities, and we are particularly indebted to Sergio Mosconi and collaborators for assistance with image processing. We thank A. Kramarz, S.M. Alvarez and L. Chornogubsky (MACN, Buenos Aires, Argentina) and M. Reguero, S.C. Scarano and M.L. de los Reyes (MLP, La Plata, Argentina), who kindly gave access to the specimens under their care. We thank the PaleoFactory Lab (Sapienza Università di Roma, Italy) for access to their facilities, without which this work would not have been possible. We also thank M. Fernández-Monescillo, S. Hernández del Pino and A. Forasiepi (IANIGLA, CCT-CONICET-Mendoza, Argenina) for their useful suggestions. This paper greatly benefited from the careful reading and thoughtful comments by the editor S. Thatje, Prof. G. De Iuliis and other two anonymous reviewers.

Funding information This research was partially funded by ECOS-FonCyT (A14U01).

References

Ameghino F (1902) Notas sobre algunos mamíferos fósiles, nuevos ó poco conocidos del valle de Tarija. Anales Mus Nac Hist Nat Buenos Aires 8:225–261

Bargo MS, Toledo N, Vizcaíno SF (2006) Muzzle of south American Pleistocene ground sloths (Xenarthra, Tardigrada). J Morphol 267: 248–263

Bargo MS, Vizcaíno SF (2008) Paleobiology of Pleistocene ground sloths (Xenarthra, Tardigrada): biomechanics, morphogeometry and ecomorphology applied to the masticatory apparatus. Ameghiniana 45(1):175–196

Benoit J, Essid EM, Marzougui W, Ammar HK, Lebrun R, Tabuce R, Marivaux L (2013) New insights into the ear region anatomy and cranial blood supply of advanced stem Strepsirhini: evidence from three primate petrosals from the Eocene of Chambi, Tunisia. J Hum Evol 65(5):551–572

Berlin JC, Kirk EC, Rowe TB (2013) Functional implications of ubiquitous semicircular canal non-orthogonality in mammals. PLoS One 8(11):e79585

Billet G, Hautier L, Asher RJ, Schwarz C, Crumpton N, Martin T, Ruf I (2012) High morphological variation of vestibular system accompanies slow and infrequent locomotion in three-toed sloths. Proc R Soc B 279:3932–3939

Billet G, Germain D, Ruf I, de Muizon C, Hautier L (2013) The inner ear of *Megatherium* and the evolution of the vestibular system in sloths. J Anat 223(6):557–567

Billet G, Hautier L, Lebrun R (2015a) Morphological diversity of the bony labyrinth (inner ear) in extant xenarthrans and its relation to phylogeny. J Mammal 96(4):658–672

Billet G, de Muizon C, Schellhorn R, Ruf I, Ladevèze S, Bergqvist L (2015b) Petrosal and inner ear anatomy and allometry amongst specimens referred to Litopterna (Placentalia). Zool J Linn Soc 173(4):956–987

Blanco RE, Rinderknecht A (2008) Estimation of hearing capabilities of Pleistocene ground sloths (Mammalia, Xenarthra) from middle-ear anatomy. J Vertebr Paleontol 28(1):274–276

Blanco RE, Rinderknecht A (2012) Fossil evidence of frequency range of hearing independent of body size in South American Pleistocene ground sloths (Mammalia, Xenarthra). C R Palevol 11(8):549–554

Clack AA, MacPhee RD, Poinar HN (2012) *Mylodon darwinii* DNA sequences from ancient fecal hair shafts. Ann Anat 194(1):26–30

Cope ED (1889) The Edentata of North America. Am Nat 23(272): 657–664

Coutier F, Hautier L, Cornette R, Amson E, Billet G (2017) Orientation of the lateral semicircular canal in Xenarthra and its links with head posture and phylogeny. J Morphol 278(5):704–717

Danilo L, Remy J, Vianey-Liaud M, Mérigeaud S, Lihoreau F (2015) Intraspecific variation of endocranial structures in extant *Equus*: a prelude to endocranial studies in fossil equoids. J Mamm Evol 22(4):561–582

David R, Droulez J, Allain R, Berthoz A, Janvier P, Bennequin D (2010) Motion from the past. A new method to infer vestibular capacities of extinct species. C R Palevol 9(6):397–410

David R, Stoessel A, Berthoz A, Spoor F, Bennequin D (2016) Assessing morphology and function of the semicircular duct system: introducing new *in-situ* visualization and software toolbox. Sci Rep 6:32772

De Iuliis G (2017) Recent progress and future prospects in fossil xenarthran studies, with emphasis on current methodology in sloth taxonomy. J Mamm Evol DOI. https://doi.org/10.1007/s10914-017-9407-8

De Iuliis G, Gaudin TJ, Vicars M (2011) A new genus and species of Nothrotheriid sloth (Xenarthra, Tardigrada, Nothrotheriidae) from the Late Miocene (Huayquerian) of Peru. Palaeontology 54(1): 171–205

De Iuliis G, Cartelle C, McDonald HG, Pujos F (2017) The mylodontine ground sloth *Glossotherium tropicorum* from the Late Pleistocene of Ecuador and Peru. Pap Palaeontol 3:613–636

Delsuc F, Catzeflis FM, Stanhope MJ, Douzery EJ (2001) The evolution of armadillos, anteaters and sloths depicted by nuclear and mitochondrial phylogenies: implications for the status of the enigmatic fossil *Eurotamandua*. Proc R Soc B 268(1476):1605–1615

Ekdale EG (2013) Comparative anatomy of the bony labyrinth (inner ear) of placental mammals. PLoS One 8(6):e66624

Ekdale EG (2016) Form and function of the mammalian inner ear. J Anat 228(2):324–337

Ekdale EG, Racicot RA (2015) Anatomical evidence for low frequency sensitivity in an archaeocete whale: comparison of the inner ear of *Zygorhiza kochii* with that of crown Mysticeti. J Anat 226(1):22–39

Ekdale EG, Rowe T (2011) Morphology and variation within the bony labyrinth of zhelestids (Mammalia, Eutheria) and other therian mammals. J Vertebr Paleontol 31(3):658–675

Esteban GI (1996) Revisión de los Mylodontinae cuaternarios (Edentata-Tardigrada) de Argentina, Bolivia y Uruguay. Sistemática, filogenia, paleobiología, paleozoogeografía y paleoecología. Dissertation, Universidad Nacional de Tucumán

Fariña RA, Vizcaíno SF, Bargo MS (1998) Body mass estimations in Lujanian (late Pleistocene-early Holocene of South America) mammal megafauna. Mastozool Neotrol 5(2):87–108

Fariña RA, Vizcaíno SF (2003) Slow moving or browsers? A note on nomenclature. Senckenb Biol 83(1):3–4

Fernicola JC, Vizcaíno SF, De Iuliis G (2009) The fossil mammals collected by Charles Darwin in South America during his travels on board the HMS Beagle. Rev Asoc Geol Argent 64(1):147–159

Flower W (1883) On the arrangement of the orders and families of existing Mammalia. Proc Zool Soc Lond 1883:178–186

Gaudin TJ (1995) The ear region of edentates and the phylogeny of the Tardigrada (Mammalia, Xenarthra). J Vertebr Paleontol 15(3): 672–705

Gaudin TJ (2004) Phylogenetic relationships among sloths (Mammalia, Xenarthra, Tardigrada): the craniodental evidence. Zool J Linnean Soc 140(2):255–305

Gaudin TJ (2011) On the osteology of the auditory region and orbital wall in the extinct west Indian sloth genus *Neocnus* Arredondo, 1961 (Placentalia, Xenarthra, Megalonychidae). Ann Carnegie Mus 80(1):5–28

Gaudin TJ, Biewener AA (1992) The functional morphology of xenarthrous vertebrae in the armadillo *Dasypus novemcinctus* (Mammalia, Xenarthra). J Morphol 214(1):63–81

Gaudin TJ, Wible JR (2006) The phylogeny of living and extinct armadillos (Mammalia, Xenarthra, Cingulata): a craniodental analysis. In: Carrano MT, Gaudin TJ, Blob RW, Wible JR (eds) Amniote paleobiology: perspectives on the evolution of mammals, birds and reptiles. University of Chicago Press, Chicago, pp 153–198

Gaudin TJ, Croft DA (2015) Paleogene Xenarthra and the evolution of South American mammals. J Mammal 96(4):622–634

Gaudin TJ, De Iuliis G, Toledo N, Pujos F (2015) The basicranium and orbital region of the early Miocene *Eucholoeops ingens* Ameghino, (Xenarthra, Pilosa, Megalonychidae). Ameghiniana 52(2):226–240

Gill T (1872) Arrangement of the families of mammals, with analytical tables. Smithson Misc Collect 11:1–98

Gosselin-Ildari AD (2006) Functional morphology of the bony labyrinth in primates. The University of Texas at Austin, Dissertation

Greenwood AD, Castresana J, Feldmaier-Fuchs G, Pääbo S (2001) A molecular phylogeny of two extinct sloths. Mol Phylogenet Evol 18(1):94–103

Guth C (1961) La région temporale des Edentés. Université de Paris, Dissertation

Illiger K (1811) Prodromus systematis mammalium et avium. C. Salfeld, Berlin

Jones MG, Spells KE (1963) A theoretical and comparative study of the functional dependence of the semicircular canal upon its physical dimensions. Proc R Soc B 157(968):403–419

van der Klaauw CJ (1931) On the tympanic region of the skull in the Mylodontidae. Proc Zool Soc Lond 1931:607–655

Lebrun R (2008) Evolution and development of the strepsirrhine primate skull. Université Montpellier II and University of Zürich, Dissertation

Lebrun R (2014) ISE-MeshTools software. http://morphomuseum.com/meshtools

Lebrun R, de León MP, Tafforeau P, Zollikofer C (2010) Deep evolutionary roots of strepsirrhine primate labyrinthine morphology. J Anat 216(3):368–380

Linnaeus C (1758) Systema naturae per regna tria naturae, secundum classes, ordines, genera, species, cum characteribus, differentiis, synonymis, locis, 10th edn, vol 1. Holmiae, Stockholm

Lydekker R (1894) The extinct edentates of Argentina. An Mus La Plata 3(2):1–118

Macrini TE, Flynn JJ, Ni X, Croft DA, Wyss AR (2013) Comparative study of notoungulate (Placentalia, Mammalia) bony labyrinths and new phylogenetically informative inner ear characters. J Anat 223(5):442–461

Malinzak MD, Kay RF, Hullar TE (2012) Locomotor head movements and semicircular canal morphology in primates. Proc Natl Acad Sci U S A 109(44):17914–17919

Manoussaki D, Chadwick RS, Ketten DR, Arruda J, Dimitriadis EK, O'Malley JT (2008) The influence of cochlear shape on low-frequency hearing. Proc Natl Acad Sci U S A 105(16):6162–6166

McAfee RK (2009) Reassessment of the cranial characters of *Glossotherium* and *Paramylodon* (Mammalia: Xenarthra: Mylodontidae). Zool J Linnean Soc 155(4):885–903

McKenna MC, Bell SK (1997) Classification of mammals above the species level. Columbia University Press, New York

Mones A (1986) Palaeovertebrata Sudamericana. Catálogo sistemático de los vertebrados fósiles de América del Sur. Parte I. Lista preliminar y bibliografía. Cour Forsch Inst Senckenberg 82:1–625

Muller M (1999) Size limitations in semicircular duct systems. J Theor Biol 198(3):405–437

Nyakatura JA (2012) The convergent evolution of suspensory posture and locomotion in tree sloths. J Mamm Evol 19(3):225–234

Orliac MJ, Benoit J, O'Leary MA (2012) The inner ear of *Diacodexis*, the oldest artiodactyl mammal. J Anat 221(5):417–426

Orliac MJ, O'Leary MA (2016) The inner ear of *Protungulatum* (pan-Euungulata, Mammalia). J Mamm Evol 23(4):337–352

Owen FRS (1840) Fossil Mammalia. In: Darwin C (ed) The zoology of the voyage of the Beagle. Smith, Elder and Co., London, pp 13–111

Owen FRS (1842) Description of the skeleton of an extinct gigantic sloth, *Mylodon robustus*, Owen, with observations on the osteology, natural affinities, and probable habits of the megatheroid quadrupeds in general. Direction of the Council, London

Patterson B, Segall W, Turnbull WD (1989) The ear region in xenarthrans (= Edentata: Mammalia). Part I. Cingulates. Fieldiana Geol 18:1–46

Patterson B, Turnbull WD, Segall W, Gaudin TJ (1992) The ear region in xenarthrans (= Edentata: Mammalia). Part II. Pilosa (sloths, anteaters), palaeanodonts, and a miscellany. Fieldiana Geol 24:1–78

Perier A, Lebrun R, Marivaux L (2016) Different level of intraspecific variation of the bony labyrinth morphology in slow- versus fast-moving primates. J Mamm Evol 23(4):353–368

Pitana VG, Esteban GI, Ribeiro AM, Cartelle C (2013) Cranial and dental studies of *Glossotherium robustum* (Owen, 1842) (Xenarthra: Pilosa: Mylodontidae) from the Pleistocene of southern Brazil. Alcheringa 37(2):147–162

Pujos F, De Iuliis G (2007) Late Oligocene Megatherioidea Fauna (Edentata: Xenarthra) from Salla-Luribay (Bolivia): new data on basal sloth radiation and Cingulata-Phyllophaga split. J Vertebr Paleontol 27(1):132–144

Pujos F, De Iuliis G, Cartelle C (2017) A paleogeographic overview of tropical fossil sloths: towards an understanding of the origin of extant suspensory sloths? J Mamm Evol 24(1):1–20

Pujos F, Gaudin TJ, De Iuliis G, Cartelle C (2012) Recent advances on variability, morpho-functional adaptations, dental terminology, and evolution of sloths. J Mamm Evol 19(3):159–169

Ruf I, Volpato V, Rose KD, Billet G, de Muizon C (2016) Digital reconstruction of the inner ear of *Leptictidium auderiense* (Leptictida, Mammalia) and north American leptictids reveals new insight into leptictidan locomotor agility. PalZ 90(1):153–171

Silcox MT, Bloch JI, Boyer DM, Godinot M, Ryan TM, Spoor F, Walker A (2009) Semicircular canal system in early primates. J Hum Evol 56(3):315–327

Sipla JS, Spoor F (2008) The physics and physiology of balance. In: Thewissen JGM, Nummela S (eds) Sensory evolution on the threshold: adaptations in secondarily aquatic vertebrates. University of California Press, Berkeley and Los Angeles, pp 227–232

Slater GJ, Cui P, Forasiepi AM, Lenz D, Tsangaras K, Voirin B, de Moraes-Barros N, MacPhee RDE, Greenwood AD (2016) Evolutionary relationships among extinct and extant sloths: the evidence of mitogenomes and retroviruses. Genome Biol Evol 8(3): 607–621

Specht M (2007) Spherical surface parameterization and its application to geometric morphometric analysis of the braincase. University of Zürich, Dissertation

Specht M, Lebrun R, Zollikofer CPE (2007) Visualizing shape transformation between chimpanzee and human braincases. Vis Comput 23(9):743–751

Spoor F, Garland T, Krovitz G, Ryan TM, Silcox MT, Walker A (2007) The primate semicircular canal system and locomotion. Proc Natl Acad Sci U S A 104(26):10808–10812

Toledo N (2016) Paleobiological integration of Santacrucian sloths (early Miocene of Patagonia). Ameghiniana 53(2):100–141

Varela L, Tambusso PS, Fariña RA (2016) Inner and middle ear 3D reconstruction of the extinct giant sloth *Lestodon armatus.* ICVM-11 abstracts, Washington DC

Vizcaíno SF, Zárate M, Bargo MS, Dondas A (2001) Pleistocene burrows in the mar del Plata area (Argentina) and their probable builders. Acta Palaeontol Pol 46(2):289–301

Wible JR (2010) Petrosal anatomy of the nine-banded armadillo, *Dasypus novemcinctus* Linnaeus, 1758 (Mammalia, Xenarthra, Dasypodidae). Ann Carnegie Mus 79(1):1–28

Wible JR, Gaudin TJ (2004) On the cranial osteology of the yellow armadillo *Euphractus sexinctus* (Dasypodidae, Xenarthra, Placentalia). Ann Carnegie Mus 73(3):117–196

Zárate MA, Bargo MS, Vizcaíno SF, Dondas A, Scaglia O (1998) Estructuras biogénicas en el Cenozoico tardío de Mar del Plata (Argentina) atribuibles a grandes mamíferos. Rev Asoc Argent Sedimentol 5(2):95–103